The International Journal of Advanced Manufacturing Technology
https://doi.org/10.1007/s00170-019-04317-6

ORIGINAL ARTICLE

Effects of silicon carbide contents on microstructure and mechanical properties of spark plasma–sintered titanium-based metal matrix

Peter Ifeolu Odetola [1] · Emmanuel Ajenifuja [1,2,3] · Abimbola P. I. Popoola [1] · Olawale Popoola [2]

Received: 10 May 2019 / Accepted: 15 August 2019

Abstract

In this study, TiNiAl-SiC composites (TMCs) containing 1, 3, and 6 wt% SiC were prepared by spark plasma sintering (SPS) process using heating rate of 100 °C/min, at 800 °C, and sintering pressure of 40 MPa, and holding time of 10 min. Phase identification was carried out on TiNiAl-SiC composites by X-ray diffraction technique. Microstructure and elemental analyses were done with a scanning electron microscope (SEM) and energy dispersive X-ray (EDS) spectroscopy. SEM micrographs showed pronounced grain boundary interaction between the SiC and the TiNiAl matrix with increase wt% SiC. The results from the mechanical characterization generally showed enhancement in hardness, tensile strength, yield strength, and wear. At 6 wt% SiC, the optimum values of 2852 MPa, 930.46 MPa, and 673.02 MPa were established for hardness, tensile strength, and yield strength, respectively. Also, TiNiAl-SiC composite with 6 wt% SiC presented the best frictional profile with the highest resisting power due to the lowest friction coefficient of about 0.4, and the wear rate of 2.18 mm^3/m. The absence of grooves in the worn morphology also confirmed that it has good tribological properties.

Keywords Titanium matrix composite · Spark plasma sintering · Powder processing · Aerospace · Microstructure · Hardness · Tensile strength · Yield strength · Wear

1 Introduction

Titanium, its alloys, and composites have metamorphosed tremendously over the years through advanced powder metallurgy, which permits flexible powder design, effective powder mixing, and synergetic processing conditions. Therefore, composite with better performance microstructurally and mechanically is now possible to be tailor-made for speciality applications under critical working conditions needed in transport industries like aerospace and automobile. Titanium has desirable properties of strength to weight ratio, moderate resistance to high-temperature oxidation, and mitigation of corrosion as a working horse material in aerospace [1–3]. From the perspective of introducing reinforcement into the matrix to form titanium matrix composites, the inherent weaknesses of titanium such as poor wear, unimpressive hardness, high reactivity, and insufficient fatigue strength at high temperatures can be addressed [4]. Reinforcement is generally a material that assists mechanical performance where it acts as a second phase. Property profiles such as hardness, high-temperature resistance, oxidation, creep, and fatigue can be easily upgraded in the material via reinforcement.

The inclusion of reinforcement material in alloy or metal matrix produces composite materials by means of synergistic component interaction. Besides considering temperature, the composition [5] also plays a role in determining hardness, toughness, and overall response to application environments. Reinforcement is always in lower weight percentage in the metal matrix composite system compared to the bulk matrix, percentage. Although present in small quantities, the overall performance properties of the materials are always pronounced. Among the carbides used as sinter additives, SiC is known by its impressive high hardness and strength fibre/ceramic properties, chemical and thermal stability, low

✉ Peter Ifeolu Odetola
odetolapeter77@gmail.com

[1] Department of Chemical, Metallurgical and Materials Engineering, Tshwane University of Technology, Pretoria West, Pretoria 0183, South Africa

[2] Center for Energy and Electric Power, Tshwane University of Technology, Pretoria, South Africa

[3] Center for Energy Research and Development, Obafemi Awolowo University, Ile-Ife, Nigeria

Published online: 31 October 2019

density, and high melting point [6–8]. Several alloys and composites of aluminium [9–11], magnesium [12], and titanium [13–17] have been satisfactorily fabricated by SiC reinforcement of their matrix [18, 19].

SiC also stands out strongly in its ability to inhibit the growth of grain and enhance the sinterability of its base materials [20–22]. Torizuka et al. 1995 successfully used SiC in the sintering process to improve the sinterability of TiB_2 by eliminating the oxide impurity layer and producing SiO_2 glassy crystal phase [23]. Comparative studies conducted by Johny et al. 2014 concluded that SiC composites have a higher hardness value than TiB_2 [24]. Poletti and Holtl 2010 established that the strengthening by SiC is due to tangible α misfit between matrix and particles. According to them, this is the reason why strengthening by SiC supersede that of TiB and TiC [14]. Barick et al. 2018 carried out comparative evaluations on the microstructural and mechanical properties of sintered silicon carbide consolidated by various techniques [25]. Spark plasma sintering (SPS) is a powder metallurgy processing technique with excellent processing conditions that accommodates the exceptionally fast heating schedule, which invariably translates into short sintering time at moderate temperature coupled with short holding time to cool down to ambient temperature the hot formed composite [26, 27]. Conditions for spark plasma sintering processing facilitate the development of composites across low and high melting point powder. Through this processing technique, temperature sensitive and insensitive powder materials can, therefore, be easily manufactured.

In this work, SiC particle-reinforced titanium matrix composites (TiNiAl-SiC) were successfully fabricated using a novel spark plasma sintering method for powder metallurgy. The effects of SiC particles additions at different weight percent composition on the microstructures and composite mechanical properties were carried out. At the highest weight percentage of SiC reinforcement (TiNiAl-6 wt% SiC), the best mechanical property profiles of hardness, tensile strength, yield strength, and wear were recorded.

2 Experimental procedure

2.1 Materials

The combined titanium, nickel, and aluminium powders were selected as matrix while silicon carbide was used as reinforcement. Figure 1 presented their initial SEM powder characterization. Table 1 presented their particle size, purity percentage, and supplier. The composition of silicon carbide and titanium were varied in the design of powders, while the composition of nickel and aluminium was kept constant in the matrix as shown in Table 2.

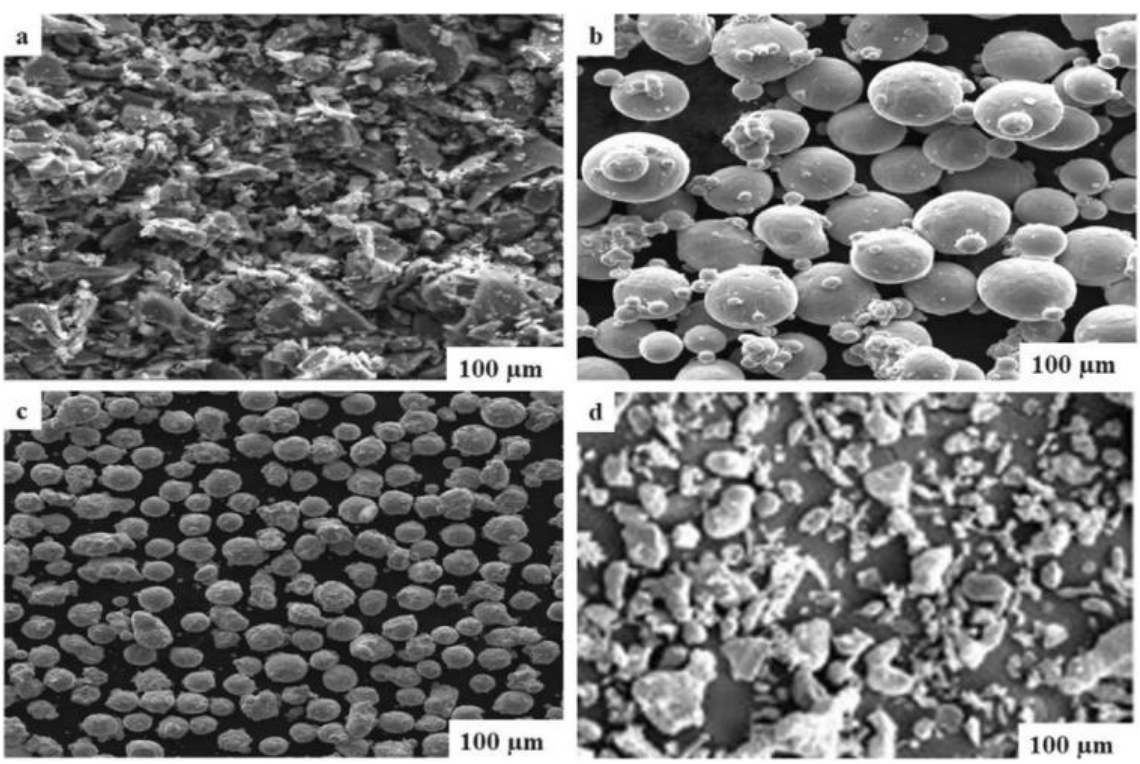

Fig. 1 SEM images of as purchased powders **a** SiC, **b** Ti, **c** Ni, and **d** Al

Table 1 Physical characteristics of the matrix and the reinforcement powders

Powders	Particle size (μm)	Purity (%)	Density (g/cm^3)	Supplier
SiC	~ 22	99.9	1.6	F.J. Brodman & Co. LLC.
Al	45–90	99.9	2.7	TLS Technik
Ni	45–90	99.9	8.9	TLS Technik
Ti	45–90	99.9	4.5	TLS Technik

2.2 Method

2.2.1 Powder preparation

The stoichiometric calculation of the matrix powders (titanium, nickel, and aluminium) and reinforcement (silicon carbide) was based on the percentage of weight as shown in Table 2. Powders were brought into homogenization by mixing in a tubular Shaker Mixer (T2F) at a stable turning speed of 72 rpm for 12 h.

2.2.2 Composites production

The SiC-reinforced TiNiAl composites were produced using the spark plasma sintering process. The premixed metal matrix and reinforcement powders were stacked into a ∅30 mm graphite die with 5 mm powder layer thickness and then sintered in SPS HPD5, FCT Systeme GmbH at a constant temperature of 100 °C, the heating rate of 100 °C/min, and the pressure of 40 MPa. TiNiAl-1% SiC, TiNiAl-3% SiC, and TiNiAl-6% SiC are the three different composites manufactured.

2.2.3 Characterizations detail

The metal matrix composite (MMC) hardness was evaluated using a Future-tech 700 microhardness tester. Before testing, specimens cut from each composite composition were polished to obtain a flat and smooth surface finish. A load of 100 gf was applied on the specimens for 15 s, and standard procedures were used to evaluate the hardness profile. Multiple hardness tests were performed on each sample, and the average value was taken as a measure of the hardness of the specimen. The TiNiAl–SiC surface morphology at varied wt% of the composite was captured using TESCAN scanning electron microscope integrated with an energy dispersive spectroscopy (EDS), which was used to examine the composite compositions.

The tensile strength and yield strength could not be demonstrated practically due to the size constraint of the SPSed specimens (∅30 mm). Their hardness values [28, 29] were calculated using the methods of Cahoon et al. 1971 and Krishna et al. 2013 respectively as represented by the following equations:

$$T_s = \frac{H}{2.9} \times \left(\frac{n}{0.217}\right)^n \quad (1)$$

$$Y_s = \left(\frac{H}{3}\right)(0.1)^n \quad (2)$$

where H is the hardness in MPa, n is the strain hardening coefficient of the material (0.15 for titanium), T is the tensile strength of the material MPa, and Y is the yield strength of the material MPa.

The various values calculated for tensile strength and yield strength from the harness values using these two aforementioned equations are presented in Table 3.

2.2.4 Tribological analysis

The tribological performances of the unreinforced titanium-based alloy and the different reinforced titanium matrix composites were analyzed under dry sliding condition using Universal Tribometer s/n RTEC 2441, USA. For 1000 s, a load of 20 N was used at a speed of 5 Hz. The samples were machined to Ø10 mm and length of 10 mm, ground, and polished to obtain smooth surfaces. The composite samples

Table 2 Mixing ratio of matrix and composite powders

Composite	Composition, wt%			
	Control	TiNiAl-1% SiC	TiNiAl-3% SiC	TiNiAl-6% SiC
SiC	–	1	3	6
Al	3	3	3	3
Ni	10	10	10	10
Ti	87	86	84	81

Table 3 Mechanical properties of TiNiAl-SiC composites

Mechanical properties	Composition (wt%)		
	1	3	6
Hardness (MPa)	2342	2595	2852
Tensile strength (MPa)	764.07	846.61	930.46
Yield strength (MPa)	552.67	612.37	673.02

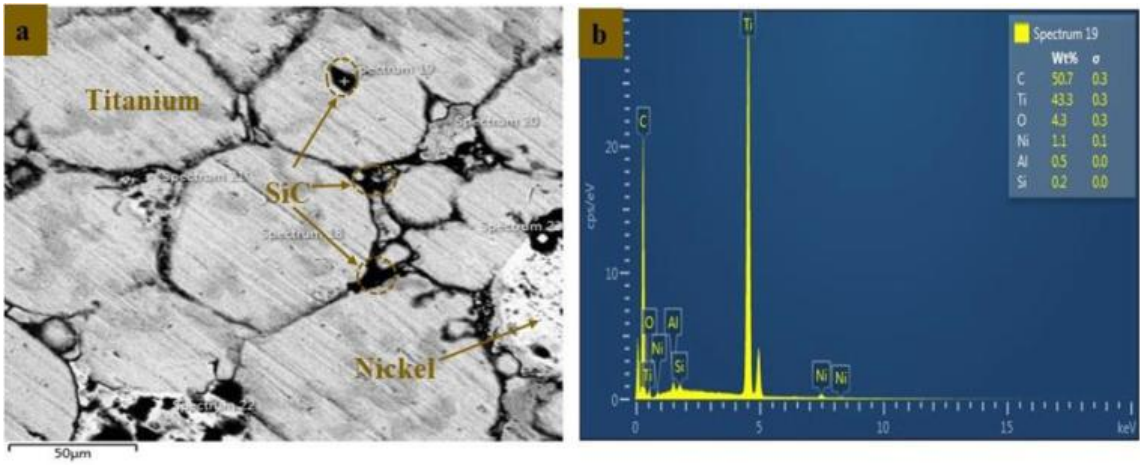

Fig. 2 Descriptive **a** microstructure and **b** EDS profile of TiNiAl-1 wt% SiC composite developed at 800 °C

were weighed to obtain the initial weight of the samples before commencing the test against hard steel alloy of 350 mm.

3 Results and discussion

3.1 Microstructure

The TiNiAl-SiC representative's microstructures and EDS mappings of the 1, 3, and 6 wt% SiC-reinforced metal matrix composites at a constant temperature of 800 °C, 40 MPa pressure, 150 °C/min heating rate, and 10-min holding time are shown in Figs. 2a, b, 3a, b, and 4a, b, respectively. In the microstructural view of TiNiAl-1% SiC at 800 °C presented in Fig. 2a, the black, grey, and white zones are the three distinct phases represented. The grey areas are dominated by titanium, while the smaller nickel layers are the scanty white globular layers. The black zones consisting of the SiC were mostly distributed within the titanium layer (the bulkiest matrix component) while the nickel layers bury a very scanty portion. There are clear grain boundaries showing regions dominated by the mixed matrix as well as atoms sparsely dispersed around the grain boundaries of the reinforcement particulates. The atomic constituents of the dissociated SiC were integrated into the matrix grains and also around the grain boundaries. These simultaneously enhance the hardness. The wt% of the reinforcement is a key to the degree of hardness induced and also influence other properties such as tensile strength and yield strength associated with it. The representative EDS in Fig. 2b of this SEM micrograph showed that SiC reinforced into the bulk titanium matrix has combine wt% influence of 0.2 wt% of Si and 50.7 wt% C (i.e. 50.9%). The composite had a minimum hardness value of 2342 MPa.

Figure 3 a and b showed the micrograph and spot analysis at 3 wt% SiC reinforcement. From the EDS view of the SEM image, it is evident that as observed from the distribution of the SiC atomic constituents over the entire microstructure, the percentage of reinforcement increased. The spot analysis showed SiC with richer phases of the constituent atoms (62 wt% Si + 32.6 wt% C). These dispersed ceramic phases have grown from the disappearing grain boundaries into the majority of the matrix, mechanically strengthening them. The

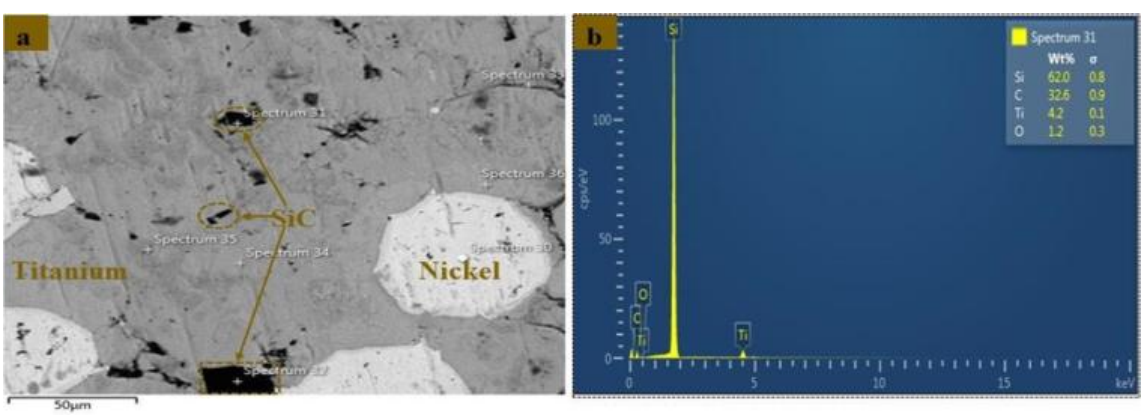

Fig. 3 Descriptive **a** microstructure and **b** EDS profile of TiNiAl-3 wt% SiC composite developed at 800 °C

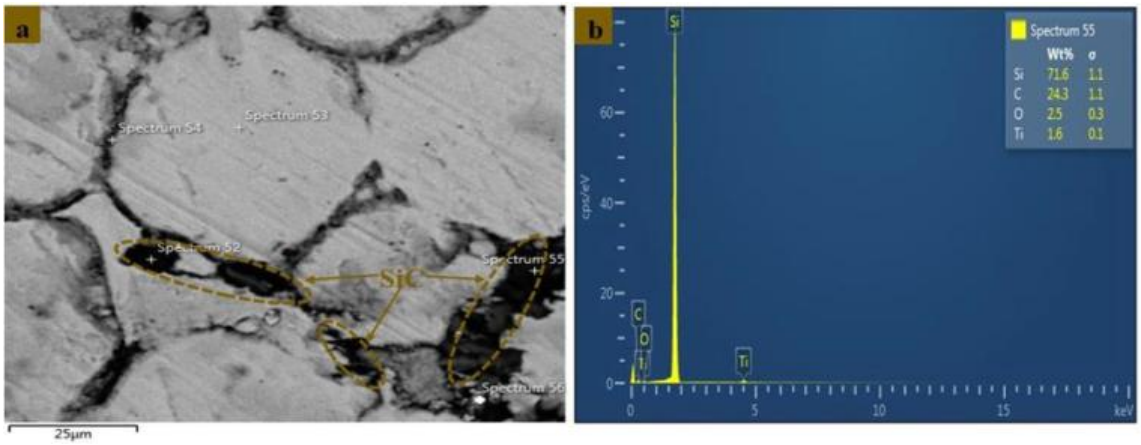

Fig. 4 Descriptive **a** microstructure and **b** EDS profile of TiNiAl-6 wt% SiC composite developed at 800 °C

combined wt% influence of the reinforcement in the matrix bulk amounts to 94.6%. This resulted in a higher hardness of 2595 MPa.

Figure 4 a and b showed the micrograph profile and EDS mapping of optimum addition of SiC to form the composite. This micrograph shows the highest constituents of the SiC (71.6 wt% Si + 24.3 wt% C). The combined wt% influence of the reinforcement in the matrix bulk amounts to 95.9% and the highest hardness value was 2852 MPa. The SEM showed rich SiC interlock zones along the boundaries of the grain. Some of the SiC has already formed intermetallic with the matrix showing the bulk matrix with a slight fade colour zones. These zones from the XRD phase composition are confirmed to be titanium matrix composite silicide compounds in various form depending on the degree of interaction that had taken place.

According to some established studies [9–17], these intermetallics are renowned reinforcements in titanium matrix composites. Equally noteworthy was the trend of atomic species of the SiC from the spot analysis was in favour of silicon while carbon depreciated gradually as seen in the composition shown in Figs. 2b, 3b, and 4b, respectively.

Figure 5 showed that the OPM of the developed TiNiAl-SiC samples viewed at a magnification of 500 displayed the

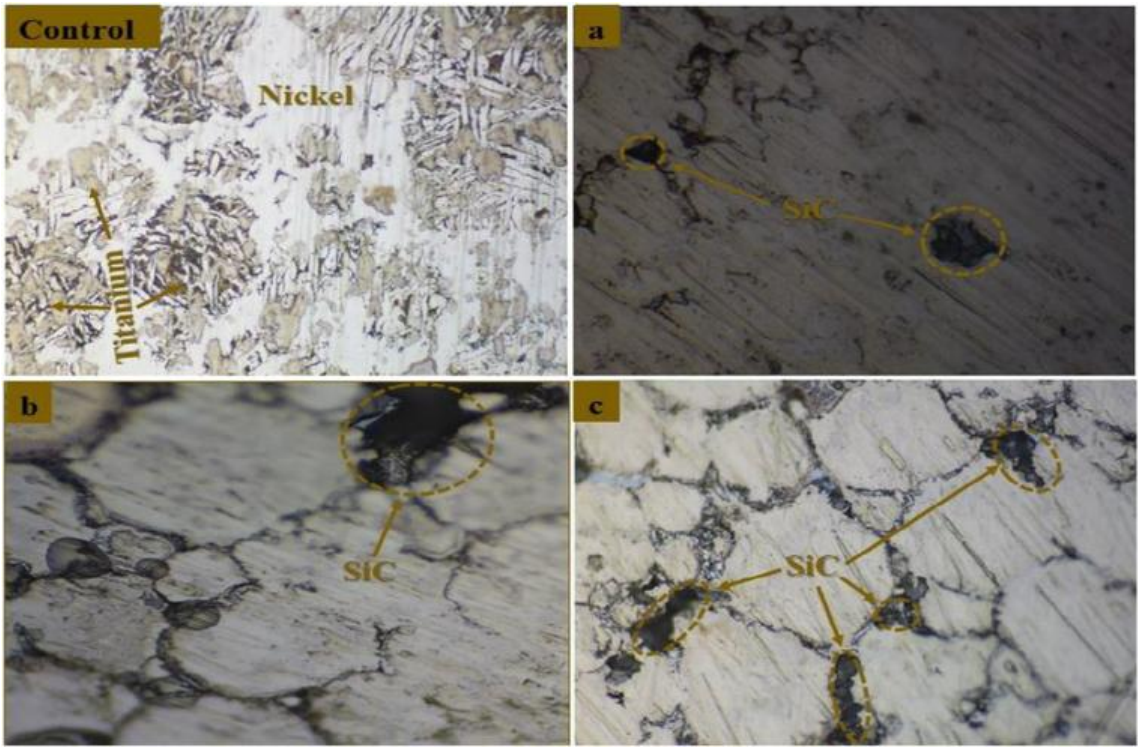

Fig. 5 OPM micrographs of control at 900 °C and TiNiAl-SiC at (a) 1 wt% (b) 3 wt%, and (c) 6 wt%

influence of SiC particulates over the entire microstructures. The control was sintered at 900 °C and no black SiC precipitate was found, but the titanium (greyish region), nickel (white region), and aluminium matrix formed different zones and phases.

Figure 5 a–c are representative 800 °C sintered OPM samples with a different weight percentage of SiC powder reinforcement. The reinforcement influence is pronounced around the grain boundaries with weight per cent increase as shown particularly in Fig. 5 (b), (c). Since the grain/grain boundary interaction between the matrix and the reinforcement is pronounced within the bulk composite, the enhanced hardness is the result of more dislocation restriction created at the interface between the matrix grain and reinforcement. This same mechanism is also responsible for enhancing yield strength and tensile strength, which is a bulk material function.

3.2 Phase XRD analysis

Figure 6 displays the control and phases present in the sinter TiNiAl-SiC composites at 1 wt% SiC, 3 wt% SiC, and 6 wt% SiC, respectively. The XRD spectra of the composites exhibit similar peaks but with different phases of intermetallic compounds at the different compositions of the reinforcement. It is evident that the reinforcement weight percentage influences the type of intermetallic identified in the spectra.

Noticeable intermetallics which features in the phases identified by the XRD are responsible for the enhanced mechanical properties at a successive increase in strengthening particles. These identified phases play a role in contributing to the mechanical properties. The intermetallic compounds identified by the phases are a varied combination of the titanium, nickel, and aluminium matrix and the SiC reinforcements such as Ti_3SiC_2, Ni (TiO_3), $Ni_4Si_7Ti_4$, Ni_2Ti_4O, $AlNi_6Si_3$, AlTiNiSi, Al_5SiC_7, and $Ni_{0.35}Al_{0.3}Si_{0.35}$. The synergetic union and contribution of individual properties of all these intermetallic in the developed TiNiAL-SiC composites make it a better material than the conventional individual matrix elements and reinforcement.

A study showed that these featured intermetallics have a good combination of properties ranging from electrical to mechanical that makes them suitable for tailored applications where retention of mechanical integrity at elevated temperature is of optimum importance. Ti_3SiC_2 intermetallic was found in the developed composites at the three different wt. per cent composition of SiC. Ti_3SiC_2 is ternary-layered carbide with a combination of metallic and ceramic properties, which makes it a proficient material with better thermal and

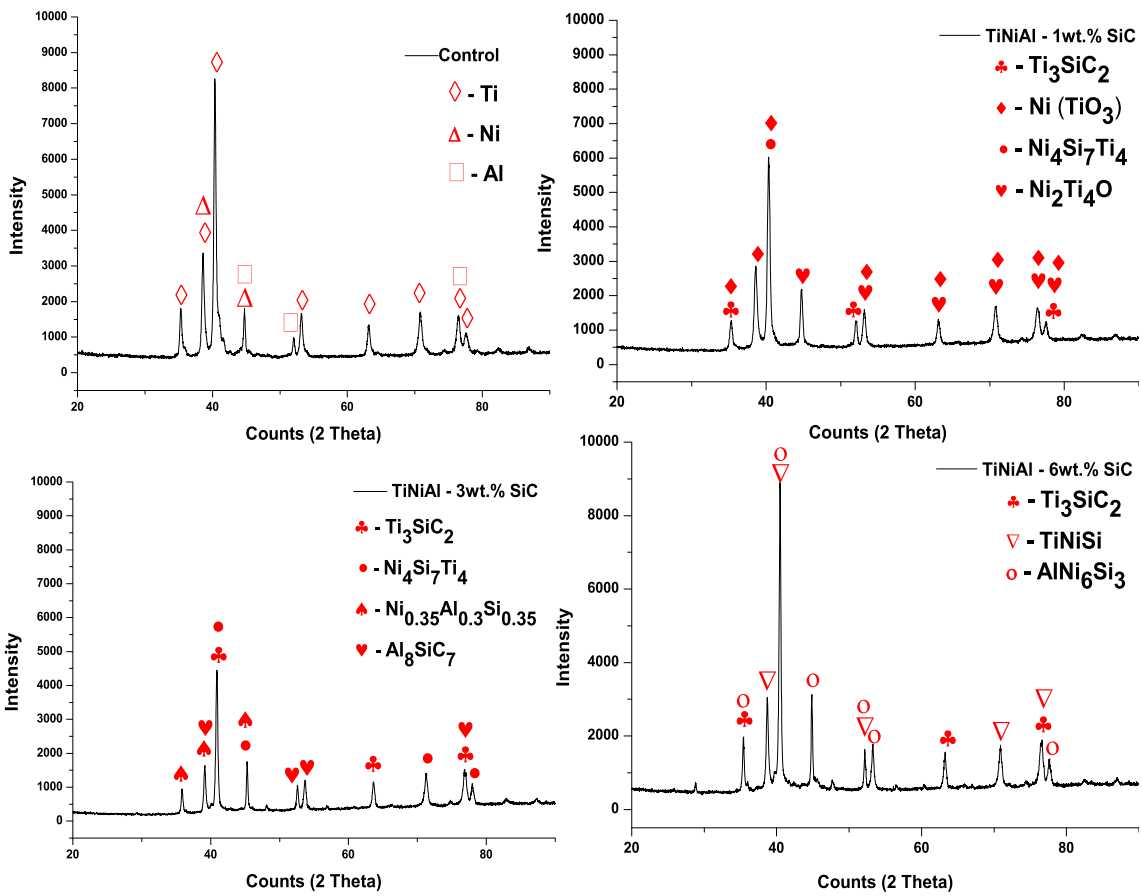

Fig. 6 XRD spectra of TiNiAl-SiC composites with different wt%

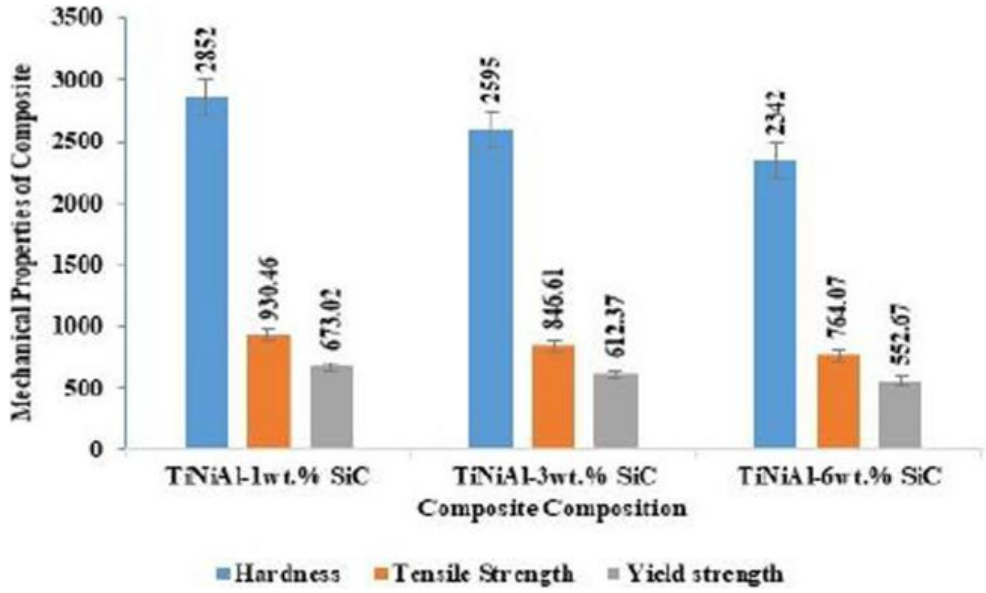

Fig. 7 Mechanical performance of TiNiAl-SiC composites at different wt%

mechanical properties than titanium metal [30, 31]. Though similar to titanium in density (4.5 g/cm^3), yet has superior resistance to thermal shock, oxidation resistant, high fracture toughness, and damage tolerance. Ti_3SiC_2 has a relatively low coefficient of thermal expansion (CTE) as well as low hardness (4 GPa) to elastic modulus ratio, which makes it readily machinable using regular high-speed tool steel with minimal or no cooling or lubrication required [32, 33].

In contrast, SiC has high hardness, a high melting point, a low coefficient of thermal expansion, high mechanical

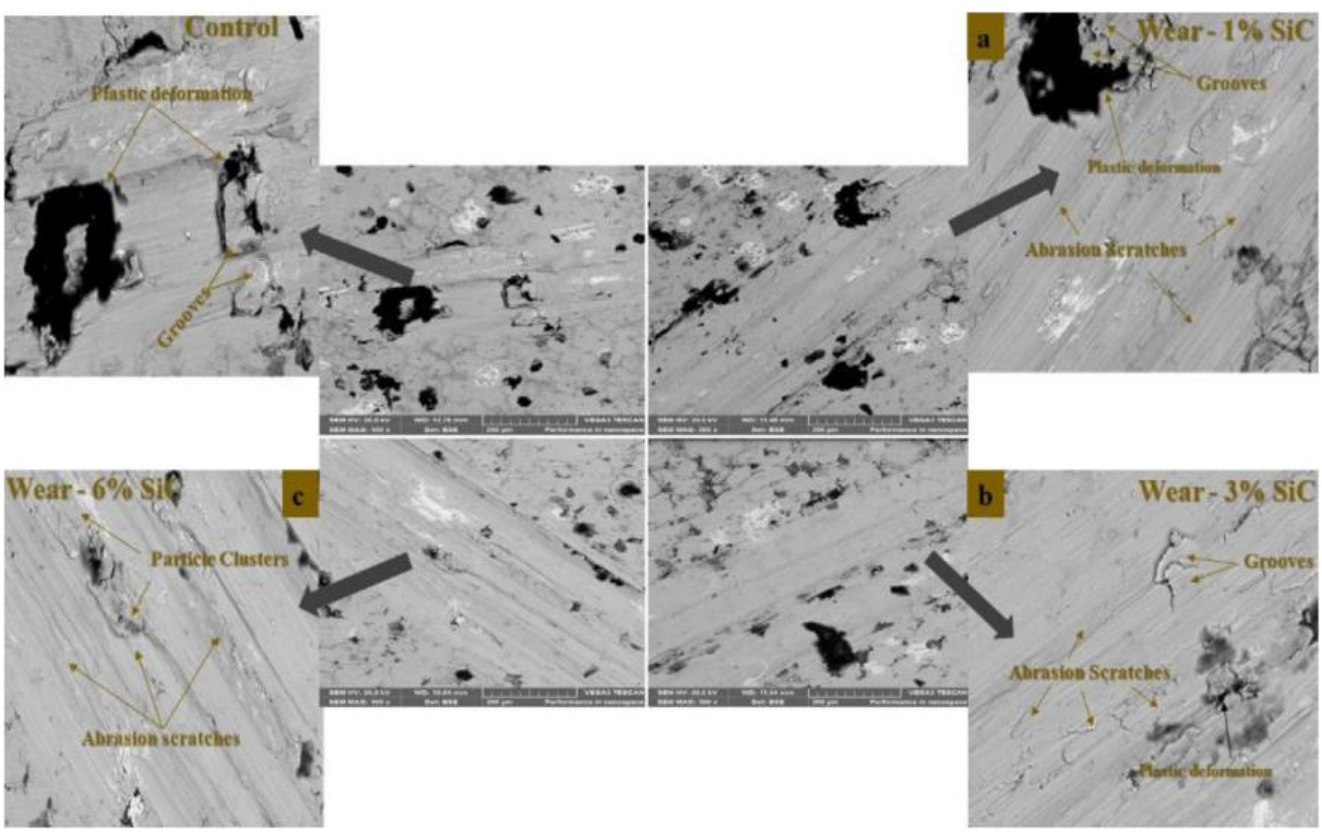

Fig. 8 SEM wear micrographs of control sample and TiNiAl-SiC at (a) 1 wt% (b) 3 wt%, and (c) 6 wt%

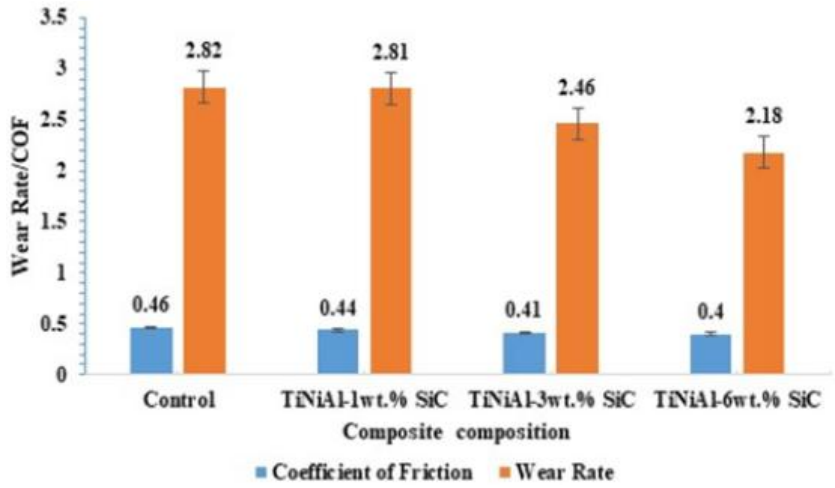

Fig. 9 Wear rate and coefficient of friction versus reinforcement composition

strength, a high elastic modulus, and low toughness [34, 35]. In some studies [36–39], Ti_3SiC_2 was combined with SiC and also with some alloys and inorganic ceramics by means of a synergetic mechanism to enhance the overall properties of the final material, making it suitable for use in harsher or more complicated conditions of service.

3.3 Microhardness

Table 3 shows that the hardness value increases as the particle composition increases from 1 to 6%. Furthermore, the enhancement of hardness of the TiNiAl-SiC composites can be attributed to the homogeneous dispersion of particles, as well as increasing the wt% of the particulates (Fig. 7). This is in correlation with Li et al. [40] and Steinman et al. [41]. At 1 wt%, 3 wt%, and 6 wt%, the minimum, intermediate, and optimum hardness level are 2342 MPa, 2595 MPa, and 2852 MPa, respectively. Between the lowest and the highest loading of the reinforcement in the developed composite, there was a significant increase in hardness up to 510 MPa. The hardness was due to the presence of the intermetallics verified from the XRD. The tensile strength and yield strength calculated from Cahoon and Krishna methods in Eqs. 1 and 2 followed the same trend as the hardness profile with subsequent enhancement as the weight percentage of SiC admixed with the matrix increases.

3.4 Wear

The same load of 20 N was used for TiNiAl-SiC composites with varied wt% of the second phase particles. The reinforcement composition controls the wear rate and coefficient of friction. Higher coefficient of friction was experienced by the unreinforced alloy (TiNiAl) for all the SPS conditions as seen in Figs. 8 and 9. Because of this higher friction coefficient, the unreinforced specimen suffered higher wear rate than the reinforced composite specimens. The wear morphologies of the composites were viewed under SEM as shown in Fig. 9. It was established that the unreinforced titanium-based alloy experienced plastic deformation due to friction and heat generation at the sliding surface. As a result, groves are much pronounced in the control sample. The presence of significant plastic deformation (worn-out) of the sample surface observed in the frictional profile was due to the absence of hard resisting particles of the reinforcement.

With a subsequent increase in the wt% of the reinforcement particles, the frictional profiles changes. At 1% SiC reinforcement shown in Fig. 8a, though little of the groves are observed, no pronounced plastic deformation occurred. Both the wear rate and the coefficient of friction got reduced showing the tangible presence of the hard resisting particles of SiC to plastic deformation, which hinders surface removal of particles and debris. In the material reinforced with 3% SiC shown in Fig. 8b, there is a presence of shallow groves and abrasion resistance due to the increase in the weight percentage of the second phase particles. In the sample reinforced with 6% SiC shown in Fig 8c, there is no evidence of groves here but more of abrasion scratches and particle clusters, which mean that this material is a better wear material against the ball penetration. In conclusion, the more the reinforcement material in the matrix of TiNiAl, the higher the resistance power of the composite.

4 Conclusion

The effects of silicon carbide contents on microstructure and mechanical properties of SPSed titanium-based metal matrix were studied across different wt% of SiC reinforcement in the titanium metal matrix (TiNiAl+1, 3, and 6 wt% SiC, respectively). The intermetallic compounds spotted out by the phases are a varied combination of the titanium, nickel, and aluminium matrix and the SiC reinforcements such as Ti_3SiC_2, Ni (TiO_3), $Ni_4Si_7Ti_4$, Ni_2Ti_4O, $AlNi_6Si_3$, AlTiNiSi, Al_5SiC_7,

and $Ni_{0.35}Al_{0.3}Si_{0.35}$. In the developed composites, the synergistic union and contribution of individual properties of all these intermetallic make it a better material than conventional individual matrix elements and reinforcement. With a subsequent population of the reinforcement particulates in the matrix network, a profound enhancement of mechanical performance was established. This was due to strong bonds formed as there are more of the reinforcements available for migration and restriction within and across the grain boundaries. At 6 wt% SiC, the optimum values of 2852 MPa, 930.46 MPa, and 673.02 MPa were established for hardness, tensile strength, and yield strength, respectively. Also, TiNiAL-SiC composite with 6 wt% SiC presented the best frictional profile with the highest resisting power due to the lowest friction coefficient of about 0.4, and the wear rate of 2.18 mm^3/m. The absence of grooves in the worn morphology also confirmed that it has good tribological properties. The spot analysis confirmed richer silicon phases and diminishing carbon phases of the constituent elements as the wt% of SiC increases, i.e. 0.2 wt% Si and 50.7 wt% C, 62 wt% Si + 32.6 wt% C, and 71.6 wt% Si + 24.3 wt% C.

Acknowledgements The authors wish to thank the Tshwane University of Technology, Pretoria, South Africa, for the logistic supports provided during the course of this work. National Research Foundation (NRF) is also acknowledged.

Funding information This work received financial support from the Tshwane University of Technology, Pretoria, South Africa.

References

1. Duncan RM, Hanson BH (1980) The selection and use of titanium. Oxford University Press for the Design Council, the British Standards Institution and the Council of Engineering Institutions https://trove.nla.gov.au/work/10014269
2. Layens C, Peters M (2003) Titanium and titanium alloys: fundamentals and applications WILEY-VCH Verlag GmbH & Co. KGaA, Weinheim
3. Banerjee D, Williams JC (2013) Perspectives on titanium science and technology. Acta Mater 61(3):844–879
4. Falodun OE, Obadele BA, Oke SR, Okoro AM, Olubambi PA (2019) Titanium-based matrix composites reinforced with particulate, microstructure, and mechanical properties using spark plasma sintering technique: a review. Int J Adv Manuf Technol 102(5–8): 1689–1701
5. Emami SM, Salahi E, Zakeri M, Tayebifard SA (2017) Effect of composition on spark plasma sintering of ZrB_2–SiC–ZrC nanocomposite synthesized by MASPSyn. Ceram Int 43(1):111–115
6. Harris GL (Ed.). (1995) Properties of silicon carbide / Gary L. Harris, editor. London: Institution of Electrical Engineers. https://trove.nla.gov.au/work/20545125
7. Pierson HO (1996) Handbook of refractory carbides and nitrides: properties, characteristics, processing and applications. William Andrew
8. Rosso M (2006) Ceramic and metal matrix composites: routes and properties. J Mater Process Technol 175(1-3):364–375
9. Fei NJ, Katgerman L, Kool WH (1994) Production of SiC particulate reinforced aluminium composites by melt spinning. J Mater Sci 29(24):6439–6444
10. Singla M, Dwivedi DD, Singh L, Chawla V (2009) Development of aluminium based silicon carbide particulate metal matrix composite. J Miner Mater Charact Eng 8(6):455–467
11. Sun C, Song M, Wang Z, He Y (2011) Effect of particle size on the microstructures and mechanical properties of SiC-reinforced pure aluminum composites. J Mater Eng Perform 20(9):1606–1612
12. Inem B, Pollard G (1993) Interface structure and fractography of a magnesium-alloy, metal-matrix composite reinforced with SiC particles. J Mater Sci 28(16):4427–4434
13. Selamat MS, Watson LM, Baker TN (2003) XRD and XPS studies on surface MMC layer of SiC reinforced Ti–6Al–4V alloy. J Mater Process Technol 142(3):725–737
14. Poletti C, Höltl G (2010) Mechanical properties of particle reinforced titanium and titanium alloys. Kovove Mater 48:87–95
15. Shamsipur A, Kashani-Bozorg SF, Zareie-Hanzaki A (2012) Fabrication of Ti/SiC surface nano-composite layer by friction stir processing. In: International Journal of Modern Physics: Conference Series, vol 5. World Scientific Publishing Company, pp 367–374
16. Ghasali E, Alizadeh M, Pakseresht AH, Ebadzadeh T (2017) Preparation of silicon carbide/carbon fiber composites through high-temperature spark plasma sintering. J Asian Ceram Soc 5(4): 472–478
17. HariKrishnan PG, Jayakumar K (2019) Synthesis and characterization of TiB 2–SiC ceramic composite produced through spark plasma sintering. In: Advances in materials and metallurgy. Springer, Singapore, pp 127–135
18. Mampuru KM, Ajenifuja E, Popoola API, Popoola O (2019) Effect of silicon carbide addition on the microstructure, hardness and densification properties of spark plasma sintered Ni-Zn-Al alloy. J King Saud Univ Sci. https://doi.org/10.1016/j.jksus.2019.01.010
19. Odetola PI, Popoola AP, Ajenifuja E, Popoola O (2019) Effects of temperature on the microstructure and physico-mechanical properties of TiNiAl-SiC composite by spark plasma sintering technique. Materials Research Express https://doi.org/10.1088/2053-1591/ab16ff
20. Perera DS, Tokita M, Moricca S (1998) Comparative study of fabrication of Si3N4/SiC composites by spark plasma sintering and hot isostatic pressing. J Eur Ceram Soc 18(4):401–404
21. Feng G, Yang Y, Zhao G, Zhang W, Luo X, Huang B (2014) Effect of hot isostatic pressing parameters on the microstructures and grain growth behavior of the matrix of SiCf/Ti-6Al-4V composites. Rare Metal Mater Eng 43(8):1839–1845
22. Asl MS, Kakroudi MG, Noori S (2015) Hardness and toughness of hot pressed ZrB2–SiC composites consolidated under relatively low pressure. J Alloys Compd 619:481–487
23. Torizuka S, Sato K, Nishio H, Kishi T (1995) Effect of SiC on interfacial reaction and sintering mechanism of TiB2. J Am Ceram Soc 78(6):1606–1610
24. James SJ, Venkatesan K, Kuppan P, Ramanujam R (2014) Comparative study of composites reinforced with SiC and TiB2. Procedia Eng 97:1012–1017
25. Barick P, Chatterjee A, Majumdar B, Saha BP, Mitra R (2018) Comparative evaluations and microstructure: mechanical property relations of sintered silicon carbide consolidated by various techniques. Metall Mater Trans A 49(4):1182–1201
26. Guillon O, Gonzalez-Julian J, Dargatz B, Kessel T, Schierning G, Räthel J, Herrmann M (2014) Field-assisted sintering technology/spark plasma sintering: mechanisms, materials, and technology developments. Adv Eng Mater 16(7):830–849
27. Abedi M, Moskovskikh DO, Rogachev AS, Mukasyan AS (2016) Spark plasma sintering of titanium spherical particles. Metall Mater Trans B 47(5):2725–2731

28. Cahoon JR, Broughton WH, Kutzak AR (1971) The determination of yield strength from hardness measurements. Metall Trans A 2(7): 1979–1983
29. Krishna SC, Gangwar NK, Jha AK, Pant B (2013) On the prediction of strength from hardness for copper alloys. J Mater 2013:1–6
30. Barsoum MW (2000) The MN+ 1AXN phases: a new class of solids: thermodynamically stable nanolaminates. Prog Solid State Chem 28(1-4):201–281
31. Ho-Duc LH (2002) Synthesis and characterization of the properties of Ti3SiC2/SiC and Ti3SiC2/TiC composites
32. Barsoum MW, El-Raghy T (1996) Synthesis and Characterization of a Remarkable Ceramic: Ti3SiC2. Journal of the American Ceramic Society, 79:1953–1956. https://doi.org/10.1111/j.1151-2916.1996.tb08018.x
33. El-Raghy T, Barsoum MW (1999) Processing and mechanical properties of Ti3SiC2: I, reaction path and microstructure evolution. J Am Ceram Soc 82(10):2849–2854
34. Kim JI, Kim WJ, Choi DJ, Park JY, Ryu WS (2005) Design of a C/SiC functionally graded coating for the oxidation protection of C/C composites. Carbon 43(8):1749–1757
35. Sedláček J, Galusek D, Riedel R, Hoffmann MJ (2011) Sinter-HIP of polymer-derived Al2O3–SiC composites with high SiC contents. Mater Lett 65(15-16):2462–2465
36. Mogilevsky P, Mah TI, Parthasarathy TA, Cooke CM (2006) Toughening of SiC with Ti3SiC2 particles. J Am Ceram Soc 89(2):633–637
37. Chen Y, Shi X, Zhai W, Deng X, Yan Z, Liu X, Lu G, Zhou H (2018) Tribological performance of Ti3SiC2 enhanced Ni3Al matrix composites. Mater Res Express 5(6):066528
38. Liu WY, Zhang JB, Jin YM, Hu TT, Chen TT, Xiao XP, Yan LM (2017) Microstructure and properties of Ti3SiC2/Al–Si composites synthesized by spark plasma sintering. Mater Res Express 4(11): 116521
39. Cui H, Zhang Y, Zhang G, Liu W, Song X, Wei N (2016) Pore and microstructure change induced by SiC whiskers and particles in porous TiB2–TiC–Ti3SiC2 composites. Ceram Int 42(7):8376–8384
40. Li RT, Dong ZL, Khor KA (2016) Al–Cr–Fe quasicrystals as novel reinforcements in Ti based composites consolidated using high pressure spark plasma sintering. Mater Des 102:255–263
41. Steinman AE, Corthay S, Firestein KL, Kvashnin DG, Kovalskii AM, Matveev AT, Sorokin PB, Golberg DV, Shtansky DV (2018) Al-based composites reinforced with AlB2, AlN and BN phases: experimental and theoretical studies. Mater Des 141:88–98